Model of a long Josephson tunnel junction including surface losses and self-pumping effect

A.L. Pankratov[1], A.S. Sobolev[2], V.P. Koshelets[2] and J. Mygind[3]

[1] Institute for Physics of Microstructures of RAS, Nizhny Novgorod, Russia
[2] Institute of Radio Engineering and Electronics, Moscow, Russia
[3] Department of Physics, Technical University of Denmark, Kgs.Lyngby, Denmark

E-mail: alp@ipm.sci-nnov.ru; sobolev@hitech.cplire.ru; valery@hitech.cplire.ru; myg@fysik.dtu.dk

Abstract. We have numerically investigated the dynamics of a long linear Josephson tunnel junction with overlap geometry (Flux-Flow Oscillator, FFO). The study is performed in the frame of a modified sine-Gordon model, which includes surface losses, self-pumping effect, and in an empirical way the superconducting gap. The electromagnetic coupling to the environment is modeled by a simple resistor-capacitor load (RC-load) placed at both ends of the FFO. In our model the damping parameter depends both on the spatial coordinate and on the amplitude of the AC voltage. In order to find the DC current-voltage curves the damping parameter has to be calculated self-consistently by successive approximations and time integration of the perturbed sine-Gordon equation. The modified model gives better qualitative agreement with experimental results than the conventional perturbed sine-Gordon model.

1. Introduction

During the last decade the flux-flow oscillator (FFO) [1] has been considered as the most promising local oscillator in superconducting integrated sub-millimeter receivers [2] and spectrometers for space-born radio astronomy and atmosphere monitoring due to its wide operational bandwidth, easy broadband tunability, and relatively high radiation power. The FFO is a long linear Josephson junction in which a viscous flow of magnetic flux quanta (fluxons) is maintained by a DC bias current and an applied DC magnetic field. The spectral linewidth of the radiation emitted from the ends of the free-running FFO is important for its ability to be frequency and phase locked. Typically, the observed free-running linewidth is 2-20MHz for an Nb-AlOx-Nb FFO in the 400-700GHz frequency range. The dynamical and fluctuational properties of the FFO has been intensively studied both experimentally and theoretically [1]-[20]. In contrast to many other types of oscillators, the FFO fluctuations are mainly caused by *internal* wideband sources, such as thermal and shot noise, that result in a spectral line of emission with nearly perfect Lorentzian shape. The power in the so-called "wings" decreases much slower with the frequency offset from the carrier than the Gaussian shaped spectral line obtained when *external* noise sources are dominant. Thus for the FFO most external noise sources can be neglected since they, on one hand are masked by the internal wideband fluctuations, and on the other hand can be compensated by frequency locking to reference oscillators or high-Q cavities. It is a pertinent fundamental and technical problem to reduce the free-running linewidth of the FFO.

In order to make an optimal FFO design we need a trustable mathematical model that includes both high and low frequency effects. However, previous theoretical attempts to reproduce the detailed behavior of the DC current-voltage characteristics (IVC) of practical FFOs were not fully successful; with given parameters one could reproduce either the steep Fiske steps or the fairly smooth flux-flow curve. The characteristic structure observed at the so-called boundary voltage due to the self-pumping effect has only been studied by Koshelets et. al. [7]. In the present paper we propose a modified sine-Gordon model which takes into account both surface losses and self-pumping effect. In order to model the electromagnetic coupling to the environment a simple resistor-capacitor load (RC-load) is placed at both ends of the FFO. Using the model we are able to calculate DC IVCs which are qualitatively similar to the experimental curves.

2. The model

For several decades the perturbed sine-Gordon model has served as the most adequate model for the long Josephson tunnel junction (JTJ), giving a good qualitative description of its basic properties such as Fiske resonances, vortices dynamics, etc.

$$\phi_{tt} + \alpha\phi_t - \phi_{xx} = \beta\phi_{xxt} + \eta(x) - \sin(\phi), \tag{1}$$

where indices t and x denote temporal and spatial derivatives, respectively. Space and time have been normalized to the Josephson penetration length λ_J and to the inverse maximum plasma frequency ω_p^{-1}, respectively, α is the damping parameter, β is the surface loss parameter, and $\eta(x)$ is the normalized DC bias current density in the so-called overlap geometry. The proper value of the surface loss parameter, β, is still unclear, but it definitely depends on voltage, so we started out from the value $\beta \approx 0.03$. The bias current density is normalized to the critical current density, and $\alpha = \omega_p/\omega_c$, where $\omega_p = \sqrt{2eI_c/\hbar C}$, $\omega_c = 2eI_cR_N/\hbar$, I_c is the critical current, C is the JTJ capacitance, and R_N is the normal state resistance.

The boundary conditions, which are related to the external DC magnetic fields, the distribution of the DC bias current, and the high frequency electromagnetic coupling to the environment, are very important. In practice the magnetic fields at the FFO ends (used as boundary conditions for the one-dimensional sine-Gordon equation) are created by a control line current running in the ground electrode along the junction. Since the magnetic field is determined by the geometry of the electrodes in the vicinity of the FFO ends the fields will not be symmetric if the topology of the electrodes asymmetric. When the FFO is used as a local oscillator in practical microwave circuits one needs to match it's low impedance at the "radiating end" ($x = 0$ in our model) to the higher impedance of eg. an SIS-mixer. The signal from the FFO is fed to the mixer via a microstrip line with impedance transformers and some filter elements. This network enables a fairly good match of the radiating end to the external environment. Usually the opposite end $x = L$ (where the chain of fluxons enters the junction) is strongly mismatched. Obviously, due to this reason the magnetic field values are different at the opposite FFO ends. These conditions were introduced into the model by choosing proper parameters of the RC-loads and magnetic field unbalance in the boundary conditions. So, we consider a JTJ with overlap geometry, where a small asymmetry is introduced as a little inline component of the current and use the following end boundary conditions (see Ref. [4])

$$\phi(0,t)_x + r_Lc_L\phi(0,t)_{xt} - c_L\phi(0,t)_{tt} + \beta r_Rc_R\phi(0,t)_{xtt} + \beta\phi(0,t)_{xt} = \Gamma - \Delta\Gamma \tag{2}$$

and

$$\phi(L,t)_x + r_Rc_R\phi(L,t)_{xt} + c_R\phi(L,t)_{tt} + \beta r_Rc_R\phi(L,t)_{xtt} + \beta\phi(L,t)_{xt} = \Gamma + \Delta\Gamma, \tag{3}$$

that simulate simple RC-loads. Γ is the normalized magnetic field, and $\Delta\Gamma = 0.05\Gamma$ is a small magnetic field difference (introduced as an experimentally motivated fitting parameter, usually, $\Delta\Gamma$ is of the order of 5-20%). The dimensionless capacitances and resistances, $c_{L,R}$ and $r_{L,R}$, are the FFO RC-load placed at the left ($x = 0$ output) and at the right ($x = L$ input) ends, respectively. Following Ref. [20], if both overlap $\eta_{ov} = (1/L)\int_0^L \eta(x)dx$ and inline $\eta_{in} = 2\Delta\Gamma/L$ components of the current are present, the total current, η_t, with respect to which all current-voltage characteristics will be computed, is the sum of overlap and inline components: $\eta_t = \eta_{ov} + \eta_{in}$.

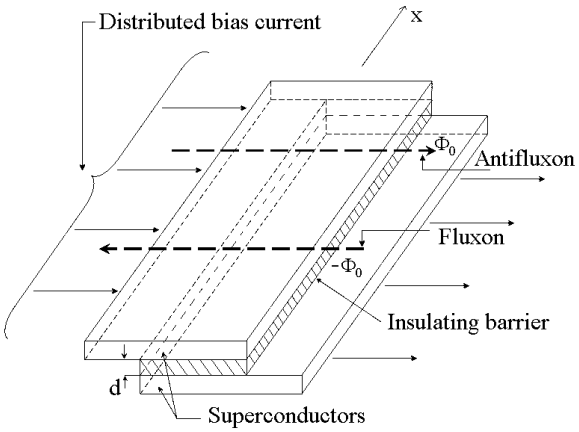

Figure 1. The structure of distributed Josephson junction of the "overlap" geometry.

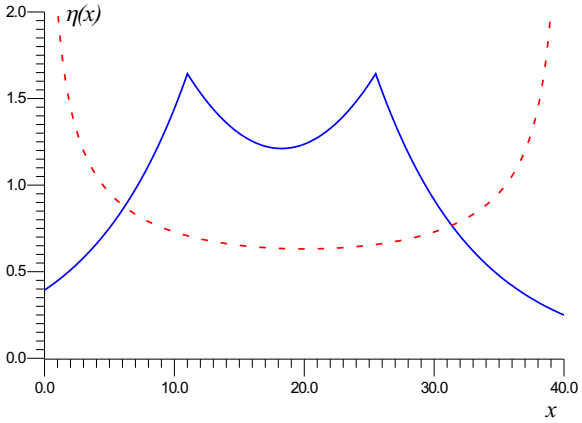

Figure 2. The distribution of overlap component of bias current $\eta(x)$. Short-dashed line: $\eta(x) = \frac{\eta_0 L}{\pi\sqrt{x(L-x)}}$; solid curve: $x_0 = 11$, $x_1 = 25.5$, $p = 0.13$, $a = 0.005$.

The profile of the DC bias current is not known and should be calculated from a three-dimensional model of the JTJ with a realistic geometry of the bias electrodes. From the experimental design one can, however, make a qualified guess on the qualitative behavior of the overlap component of bias current profile, e.g., the positions of the two maxima for this function are located at the edges of the current injector electrode. As a qualified guess let us assume the current profiles depicted in Fig.2. Since the JTJ is long compare to its width, one can use, as a first approximation, the current profile known for a superconducting film: $\eta(x) = \frac{\eta_0 L}{\pi\sqrt{x(L-x)}}$ (see, e.g., Ref. [21]), where L is the dimensionless length of the JTJ and η_0 is a constant given by the total overlap component of the current in the film. In order to describe also the situation where the width of the bias electrodes is smaller than the junction length (as it was realized in some experimental designs), let us consider the current profile, depicted in Fig.2 by the solid curve. Here we assumed, that the current profile is parabolic (with the curvature $a = 0.005$ in Fig. 2) between the left and the right boundaries of the bias electrode x_0 and x_1 ($0 \le x_0 \le x \le x_1 \le L$), and drops down exponentially in the unbiased tails $x \le x_0$, $x \ge x_1$ with the decay factor p: $\exp(-px)$ (with $p = 0.13$ in Fig. 2). The decay factor and the parabolic curvature will be used as fitting parameters when we make a comparison with the experimental IVCs.

3. Influence of surface losses on current-voltage characteristics

First, we investigate the conventional sine-Gordon model including the surface losses term $\beta\phi_{xxt}$, as given by Eq. (1). To solve Eq. (1) numerically, we have used the implicit difference scheme, described, e.g., in [22]. If the model parameters are selected close to the experimental ones the

numerical simulations of Eq.(1) give a reasonably good qualitative agreement with the measured IVCs (i.e. the dependence of the time-averaged dimensionless voltage $v(t) = d\phi/dt$ on the total bias current $\eta_t = \eta_0 + 2\Delta\Gamma/L$, $\eta_0 = (1/L)\int_0^L \eta(x)dx$) (see Fig.3). The JTJ length is $L = 40$, $\alpha = 0.033$, $\beta = 0.035$, $c_L = c_R = 10$, $r_L = 2$, $r_R = 100$, the polarity of the bias current and the magnetic field Γ are chosen such that the fluxon chain moves from right to left.

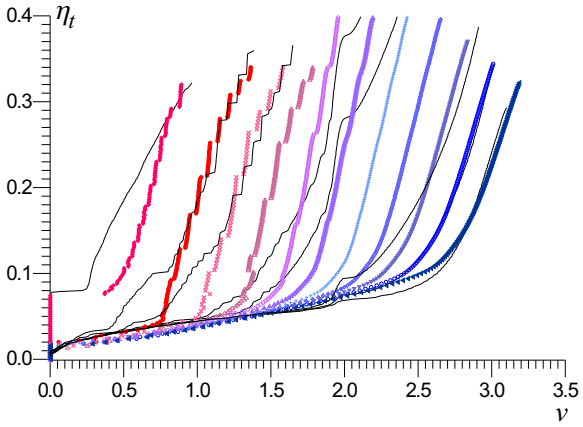

Figure 3. A series of DC current-voltage characteristics each obtained for incremented values (from left to right $\Gamma = 1.85; 2.0; 2.2; ...; 3.6; 3.8$) of the external magnetic field for the following parameters: $L = 40$, $\alpha = 0.033$, $\beta = 0.035$, $c_L = c_R = 10$, $r_L = 2$, $r_R = 100$. Thin lines - experimental measurements. Numerical simulations: triangles, crosses, circles, etc., for the current profile, depicted in Fig. 2 by the solid line.

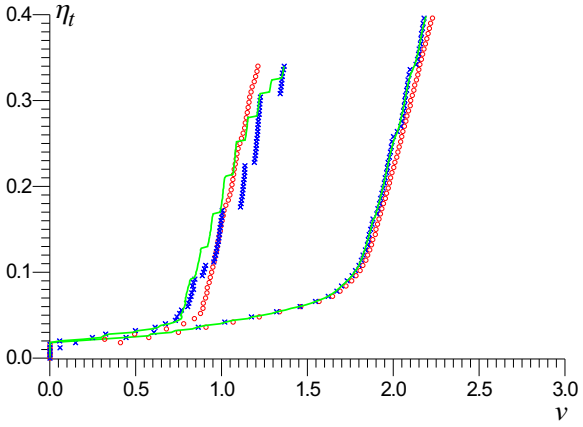

Figure 4. Calculated current-voltage characteristics of the FFO. Numerical simulations for different values of the load; crosses - unloaded symmetrical case, thin lines - asymmetric load $r_L = 2$, $r_R = 100$, circles - perfect matching $r_L = r_R = 1$, all other parameters are the same as used for the IVCs in Fig.3.

A typical set of experimental IVCs at different fixed values of the magnetic field for an Nb-AlOx-Nb FFO is shown in Fig.3 (thin solid lines). In this figure the experimental data are represented in the normalized units valid for Eq.(1). In order to convert units correctly we need to know the total critical current I_c of the junction and ω_p, as the DC voltage has to be finally normalized to $\omega_p\hbar/2e$. We took $I_c = 0.72 \cdot \delta Ig$ and $\omega_p = C_{SW}/\lambda_J$, where C_{SW} is the Swihart velocity and δIg is the jump of the quasiparticle current at the superconducting gap voltage v_g. In the experiment these parameters had the following values: $I_c = 243mA$, $\omega_p = 1.28 \cdot 10^{12}Hz$. It gives the normalized value of v_g equal to 5.7. The so called "boundary voltage", which is 1/3 v_g clearly divides the family of IVCs into two regions with a boundary at $v_b = 1.9$. Below v_b the IVC consists of nearly vertical, equally spaced voltage spikes, the so-called Fiske steps, which are due to electromagnetic resonances (Fiske resonances) in the JTJ. Above v_b the damping parameter is drastically increased due to the so-called self-pumping effect [7], which is explained as a resonant tunneling of quasiparticles similar to the well known photon assisted tunneling, PAT. As it was shown in [7], the self-pumping results in an increase of the quasiparticle current and accordingly the shunt damping α. This results in a broadening of the resonant Fiske steps and a transformation of the IVC into the smooth so-called flux-flow curve. For $v > v_b$ continuous tuning of the FFO frequency is possible and for fixed bias current the junction DC voltage increases approximately proportional to the magnetic field.

However, as it follows from Fig.3, even without accounting for the self-pumping effect, but with the surface losses included, one can see the same IVCs behavior: smoothing at higher

oscillation frequency. It leads to a qualitative coincidence between the experimental and theoretical results for the bias current profile, depicted in Fig.2 by the solid line. It is known, that it is very difficult to numerically calculate the IVC for a long JTJ with small damping, i.e. in the region with steep Fiske steps (voltage spaced as π/L). Usually, the solution gets locked around one step and it is only possible to "jump" to neighboring steps by, e.g., changing the initial conditions. In the present case, however, all the Fiske steps could be calculated using a continuous change of bias current, probably due to the account of surface losses, which makes the curves smoother.

4. Influence of RC load on current-voltage characteristics

In Fig.4 we have calculated the effect of the high frequency load on the Fiske steps using the same parameters and current profile as for the IVCs shown in Fig.3. First the almost unloaded symmetric case, $r_L = r_R = 100$ (crosses in Fig.4), the Fiske steps extend to higher currents and seem to have larger voltage spacing (sometimes even by the separation $2\pi/L$) when compared to the asymmetric case with $r_L = 2$, $r_R = 100$ (solid lines). Secondly, with a perfect match at both ends ($r_L = r_R = 1$ - circles) the Fiske steps disappear almost completely, see the curve for $\Gamma = 2$. The same behavior is observed also for larger magnetic field $\Gamma = 2.8$, the only difference being that the Fiske steps are smoother due to the surface losses.

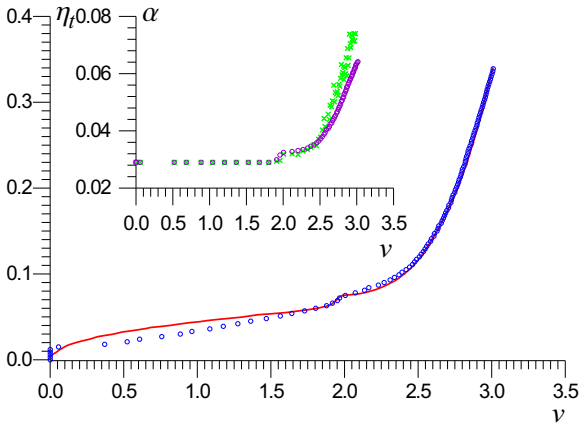

Figure 5. Current-voltage characteristics of the FFO. Thin line - experimental measurements. Numerical simulations including the self-pumping effect - circles. Inset: the damping $\alpha(x)$ at the middle of the junction (crosses) and spatially averaged (circles).

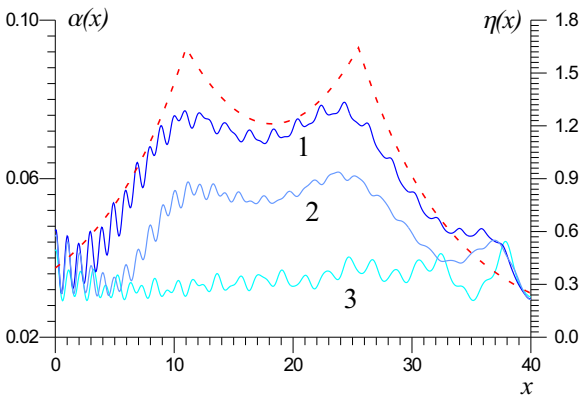

Figure 6. Spatial dependence of the shunt damping $\alpha(x)$ for three currents η_t; $\Gamma = 3.7$: curve 1 - η_t=0.3, curve 2 - η_t=0.2, curve 3 - η_t=0.1. The dashed line represents the distribution of $\eta(x)$.

5. Including the self-pumping effect

In order to give a better description of the experimental situation one should incorporate into the sine-Gordon model the self-pumping effect, with α being defined self-consistently from the amplitude of the AC-voltage. If we start from the unpumped DC IVC, $\eta_t(v_{dc})$, and apply a high-frequency signal, so the total voltage across the junction is $v(t) = v_{dc} + v_{ac}\cos(\omega t + \psi)$, then, according to [23], the total DC quasiparticle tunneling current η_{pump} of the pumped junction will be given by

$$\eta_{pump}(v_{dc}, \omega, v_{ac}) = \sum_{n=-\infty}^{n=+\infty} J_n^2\left(\frac{ev_{ac}}{\hbar\omega}\right)\eta_t(v_{dc} + n\hbar\omega/e), \qquad (4)$$

where J_n are Bessel functions of n'th order. One can use this formula for the photon assisted tunnelling (PAT) of quasiparticles to take into account the self-pumping effect by treating the Josephson radiation as an external signal. Therefore, if we take $v_{dc} = \hbar\omega/2e$ and the parameter α (which has to be dependent on the coordinate x) as the ratio η_{pump}/v_{dc}, we get $\alpha = \eta_{pump}(v_{ac}(x), x)/v_{dc}$. In our simulations we took $\eta_t(v_{dc})$ of the unpumped FFO following the nonlinear resistive model as (see [24], formula (2.27)):

$$\eta_t = \alpha_0 v \left\{ b\frac{(v/v_g)^n}{((v/v_g)^n + 1)} + 1 \right\}.$$

Here the factor $b = R_j/R_n = 35$ (compare with $b = R_j/R_n = 25$ in Ref. [7]) is the ratio between the normal state resistances below and above the gap voltage. The power index n may be taken from 10 to ∞, while we took $n = 80$, however, there were no visible difference between calculated curves for n ranging from 20 to 80.

With these modifications the self-pumped IVC can be numerically computed using the iterative procedure combined with the implicit difference scheme for the solution of Eq. (1). Namely, at the first step the AC voltage of JTJ with a certain initial value of α is calculated. At the second step the obtained AC voltage $v_{ac}(x)$ is considered to pump the JTJ. Here the damping $\alpha(x) = \eta_{pump}(v_{ac}(x), x)/v_{dc}$ is computed. This procedure is repeated with a new $\alpha(x)$ until the steady-state value of v_{dc} is found with a desired precision. The IVC obtained by this approach is shown in Fig.5 (circles). It has a step-like peculiarity on the foot of the curves at the "boundary voltage", similar to that observed for the experimentally measured IV-curves (Fig.5, thin lines, see also the same peculiarity for $\alpha(v)$ in the inset). The curve is computed for almost the same parameters as in Fig.3, and $\Gamma = 3.7$, $L = 40$, $\beta = 0.04$, $c_L = c_R = 10$, $r_L = 2$, and $r_R = 100$.

In spite of the nearly perfect agreement between the numerically computed curve and the experimental curve, it should be noted, that formula Eq.(4) is valid only for small driving amplitudes, and the curves, calculated for large self-pumping steps demonstrate unstable behavior. To extend our analysis for arbitrary values of the self-pumping steps one should either use a more exact formula instead of (4) or even consider a more general integral equation instead of the sine-Gordon equation (1). Nevertheless, the presented approach allows us to perform the analysis of the self-pumping effect, and, in particular, to study the dependence of ohmic losses versus the DC voltage and the spatial coordinate x. The inset of Fig.5 shows the damping $\alpha(x)$ in the middle of the junction (crosses) and averaged over the coordinate x (circles). The damping increases significantly (up to 3 times) for voltages above $v_b = 1.9$ as predicted in Ref.[7]. In difference with Ref.[7], in the inset of Fig. 4 α is considered in a large scale, so if one cuts the curves up to voltages 2.4, and consider in more detail the currents below 0.04, one will see the same qualitative behavior of α as in Ref. [7], with the only exception, the we do not observe the small step at $v_g/5$, since we consider pumping the FFO by its own radiated signal, which is rather small for small currents/voltages, while in Ref. [7] this pumping was considered to have constant amplitude independent of the junction's biasing point. The functions $\alpha(x)$ for the three total bias current values η_t (calculated for the corresponding voltages of Fig.5) are shown in Fig.6 together with the distribution of the applied bias current $\eta(x)$. It is seen, that $\alpha(x)$ increases with increasing overlap bias current density $\eta(x)$, and this effect is even more pronounced for large voltages, where the self-pumping effect increases.

6. Conclusions

The present paper contains an analysis of the nonlinear dynamics of a long overlap Josephson tunnel junction in the frame of a modified sine-Gordon model which takes into account surface losses and RC load at both ends of the junction. It is demonstrated that the qualitative behavior

of the DC current-voltage characteristics of a real Flux-Flow Oscillator may be reproduced using a realistic set of junction and bias parameters. In particular, the transition from the I-V curve with steep and narrow voltage spaced Fiske steps to the smooth I-V curve in the flux-flow region may be explained by the surface losses and the self-pumping effect. It was shown that the self-pumping effect may increase the ohmic losses up to 3 times, which in turn leads to additional smoothing of the I-V curves. The obtained results give us the hope that the use of more advanced models will allow for a very detailed prediction of the I-V characteristics of practical FFOs.

Acknowledgments

The authors wish to thank E. Goldobin for fruitful discussions.

The work was supported by the RFBR project 06-02-17206, ISTC project 3174, NATO SfP Grant 981415, the President Grant for Leading Scientific School 7812.2006.2, CSTP contract N 02.442.11.7342, the Danish Natural Science Foundation, and the Hartmann Foundation.

References

[1] Nagatsuma T, Enpuku K, Irie F and Yoshida K, 1983 *J. Appl. Phys.* **54** 3302, see also Pt. II: ibid. 1984 **56** 3284; Pt. III: ibid., 1985 **58** 441; Pt. IV: ibid. 1988 **63**, 1130.
[2] Koshelets V P and Shitov S V, 2000 *Supercond. Sci. Technol.* **13** R53.
[3] Koshelets V P, Shchukin A, Lapytskaya I L and Mygind J 1995 *Phys. Rev.* B **51** 6536.
[4] Soriano C, Costabile G and Parmentier R D 1996 *Supercond. Sci. Technol.* **9** 578.
[5] Golubov A A, Malomed B A and Ustinov A V 1996 *Phys. Rev.* B **54** 3047.
[6] Ustinov A V, Kohlstedt H and Henne P 1996 *Phys. Rev. Lett.* **77** 3617.
[7] Koshelets V P, Shitov S V, Shchukin A V, Filippenko L V, Mygind J and Ustinov A V 1997 *Phys. Rev.* B **56** 5572.
[8] Betenev A P and Kurin V V 1997 *Phys. Rev.* B **56** 7855.
[9] Cirillo M, Grønbech-Jensen N, Samuelsen M R, Salerno M and Rinati G V 1998 *Phys. Rev.* B **58** 12377.
[10] Salerno M and Samuelsen M R 1999 *Phys. Rev.* B **59** 14653.
[11] Mortensen U, Salerno M and Samuelsen M R 2001 *Phys. Lett.* A **285** 350.
[12] Salerno M, Samuelsen M R and Yulin A 2001 *Phys. Rev. Lett.* **86** 5497.
[13] Pankratov A L 2002 *Phys. Rev.* B **65** 054504.
[14] Pankratov A L 2002 *Phys. Rev.* B **66** 134526.
[15] Koshelets V P, Shitov S V, Dmitriev P N, Ermakov A B, Filippenko L V, Khodos V V, Vaks V L, Baryshev A M, Wesselius P R and Mygind J 2002 *Physica* C **367** 249.
[16] Koshelets V P, Dmitriev P N, Sobolev A S, Khodos V V, Pankratov A L, Vaks V L, Baryshev A M, Wesselius P R and Mygind J 2002 *Physica* C **372-376** 316.
[17] Shitov S V, Koshelets V P, Ermakov A B, Dmitriev P N, Filippenko L V, Khodos V V, Vaks V L, Yagoubov P A, Vreeling W-J and Wesselius P R 2003 *IEEE Trans. Appl. Supercond.* **13** 684.
[18] Koshelets V P, Shitov S V, Ermakov A B, Filippenko L V, Koryukin O V, Khudchenko A V, Torgashin M Yu, Yagoubov P, Hoogeveen R and Pylypenko O M 2005 *IEEE Trans. Appl. Supercond.* **15**, 960.
[19] Koshelets V P, Dmitriev P N, Ermakov A B, Sobolev A S, Torgashin M Yu, Kurin V V, Pankratov A L and Mygind J 2005 *IEEE Trans. on Appl. Supercond.* **15** 964.
[20] Mygind J, Koshelets V P, Samuelsen M and Sobolev A S, 2005 *IEEE Trans. on Appl. Supercond.* **15**, 968.
[21] Samuelsen M R and Vasenko S A 1985 *J. Appl. Phys.* **57** 110.
[22] Zhang Y 1991 *Theoretical and experimental studies of the flux-flow type Josephson oscillator*, PhD thesis, Chalmers University of Technology, 57 p.
[23] Tucker J R and Feldman M J 1985 *Rev. Mod. Phys.* **57** 1055.
[24] Likharev K K 1986 *Dynamics of Josephson Junctions and Circuits* (New York: Gordon and Breach).